DE GRUYTER Z. Naturforsch. 2016; 71(8)a: 731–734

Elena V. Nikolaeva*, Irina D. Zakiryanova, Andrey L. Bovet and Iraida V. Korzun

On Barium Oxide Solubility in Barium-Containing Chloride Melts

DOI 10.1515/zna-2016-0163
Received April 22, 2016; accepted May 29, 2016; previously published online June 24, 2016

Abstract: Oxide solubility in chloride melts depends on temperature and composition of molten solvent. The solubility of barium oxide in the solvents with barium chloride content is essentially higher than that in molten alkali chlorides. Spectral data demonstrate the existence of oxychloride ionic groupings in such melts. This work presents the results of the BaO solubility in two molten $BaCl_2$–NaCl systems with different barium chloride content. The received data together with earlier published results revealed the main regularities of BaO solubility in molten BaO–$BaCl_2$–MCl systems.

Keywords: Barium Oxychloride; Liquidus Temperature; Raman Spectroscopy; Solubility; Thermal Analysis.

1 Introduction

Oxide admixtures in molten chlorides essentially affect properties of electrolyte such as liquids temperatures, viscosity, and electroconductivity [1–5]. Mixtures of molten alkali metal chlorides and barium chloride can be used as electrolytes in process of barium and its alloys production [6]. The motivation of this article was to establish the BaO solubility and the mechanism of oxide dissolution in molten solvents of interest for the synthesis of nano powders of the barium and rare-earth metal complex oxides [7].

It is well known that oxide solubility in chloride melts depends on temperature and composition of molten solvent. It reaches maximum when the ionic potential of the oxide cation coincides with that of the solvent-salt cation [8]. That is why the solubility of barium oxide in the solvents containing barium chloride is essentially higher than that in molten alkali chlorides [6–12]. Spectral data [12, 13] demonstrate the existence of oxychloride ionic groupings in such melts.

We have previously studied the BaO dissolution process in molten $0.27BaCl_2$–0.73KCl [7] and $0.27BaCl_2$–0.36NaCl–0.37KCl [12] eutectics. The type, structure, and composition of oxychloride groupings were determined *in situ* in molten BaO–$BaCl_2$–NaCl–KCl system by Raman spectroscopy [12]. The oxide dissolution was found to proceed according to the chemical mechanism:

$$\begin{aligned}&BaO(solid)+[BaCl_6^{4-}+4M^+](solution)=\\&\quad[Ba_2OCl_6^{4-}+4M^+](solution),\end{aligned}\qquad(1)$$

where M – Na or K.

In this regard, the increasing in the barium oxide solubility with the growth of barium chloride concentration in the melt is clarified: the larger content of barium-containing chloride ionic groupings $[BaCl_6]$ results in larger content of "construction material" for oxychloride groupings $[Ba_2OCl_6]$. In addition, the ionic potential of alkali metal in $BaCl_2$–MCl molten solvent should affect the stability of the initial chloride and generated oxychloride ionic groupings and, respectively, the BaO solubility.

This work presents the results of the BaO solubility in molten $BaCl_2$–NaCl systems with different barium chloride content. The received data together with our earlier published results [7, 12] revealed the main regularities of BaO solubility in molten BaO–$BaCl_2$–MCl systems.

2 Experimental Section

Chemically pure grade NaCl (99.9 %) and $BaCl_2$ (99.5 %) ("Vekton," St. Petersburg, Russian Federation) were used. Barium oxide was prepared before each experiment from barium nitrate (99.5 %) ("Vekton," St. Petersburg, Russian Federation) using the well-known technique [14].

The DSC studies were carried out using the STA 449C Jupiter® thermal analyser produced by NETZSCH Company (Germany). The Raman spectra were recorded using the optic fiber spectrometric Ava-Raman complex (Avantes, The Netherlands), which includes the monochromatic laser (λ = 532 nm, radiation power of 50 mW). The methods of salt preparation, liquidus temperature measuring, and the high-temperature Raman spectra analysis were described in detail in our previous works [7, 12].

***Corresponding author: Elena V. Nikolaeva,** Institute of High Temperature Electrochemistry, Ural Federal University, Yekaterinburg, Russian Federation, E-mail: E.Nikolaeva@ihte.uran.ru
Irina D. Zakiryanova and Andrey L. Bovet: Institute of High Temperature Electrochemistry, Ural Federal University, Yekaterinburg, Russian Federation
Iraida V. Korzun: Institute of High Temperature Electrochemistry, Yekaterinburg, Russian Federation

3 Results and Discussion

The melting temperature of the $0.40BaCl_2–0.60NaCl$ eutectic (926 ± 5 K) defined by the cooling curve analysis agrees with literature data (927 K) [15]. The measurements carried out by the DSC method showed that the eutectic melting temperature was 928 ± 1 K. The liquidus temperature of the double system $0.27BaCl_2–0.73NaCl$ was found to be equal 1003 ± 5 K.

The dependence of liquidus temperatures on the added barium oxide concentration is shown in Figure 1. At first, the BaO additions decrease the temperature of initial crystallisation and then increase it. Experimental results for earlier studied barium-containing oxide-chloride melts [7, 12] were the similar. The change of the dependence flow may be due to the new solid phase which was the first to crystallise during the melt cooling. The increasing portion of liquidus temperature curve in Figure 1 corresponds to the barium oxide solubility (*S*).

The solubility values thus obtained may be approximated by the (2) in the temperature range under study:

$$\ln S = A + B/T. \tag{2}$$

where *A* and *B* are the empirical coefficients. Table 1 shows the *A* and *B* values for $BaCl_2–NaCl$ systems under study together with earlier published results [7, 12]. The BaO solubility in molten $0.40BaCl_2–0.60NaCl$ eutectic is larger than that in molten $0.27BaCl_2–0.73NaCl$ system at the same temperature. This fact agrees well with the literature data. The BaO solubility in the molten $NaCl–KCl–BaCl_2$ mixtures increases at 973 K from 0.77 to 10.94 mol.% with increasing of $BaCl_2$ content from 5 to 55 mol.% [11]. The similar tendency was observed by Boghosian et al. [10] in the $NaCl–BaCl_2$ melts.

Figure 2 illustrates the temperature dependence of BaO solubility in $BaCl_2–MCl$ solvents with the same (0.27 mole fraction) barium chloride concentration. It is obvious that substitution of potassium chloride on sodium chloride results in slightly reduction of the barium oxide solubility. The solubility values in molten $BaCl_2–NaCl–KCl$ [12] eutectic agree well with data [11] determined by isothermal saturation method (Fig. 2, curve 4).

The Gibbs energy changes during the BaO dissolution can be expressed by (3).

$$\Delta\bar{G}^* = -RT\ln k^* = -RT\ln S \tag{3}$$

where k^* is the conditional equilibrium constant of the reaction: BaO(solid) ↔ BaO(solution), with the assumption that the barium activity coefficients in chloride and oxychloride groupings are unchangeable in the concentration range under study.

Substitution of (2) to (3) gives the following equation for temperature dependence of the Gibbs energy changes:

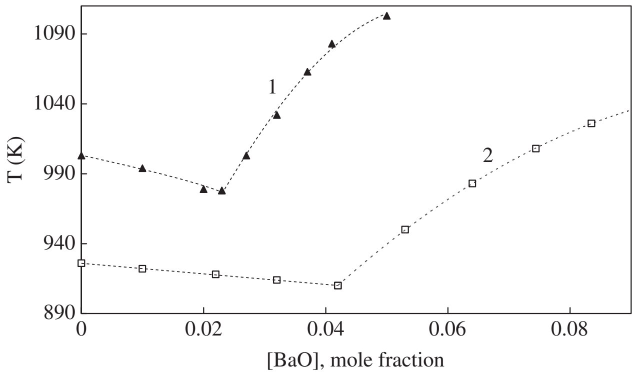

Figure 1: Liquidus temperatures of molten systems: $BaO–[0.27BaCl_2–0.73NaCl]$ (1); $BaO–[0.40BaCl_2–0.60NaCl]$ (2).

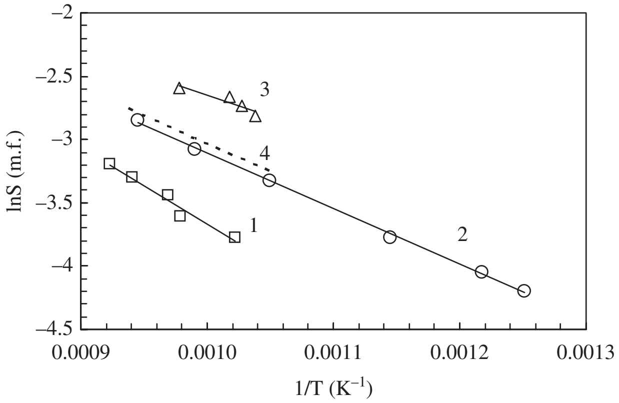

Figure 2: Temperature dependence of BaO solubility in molten chloride systems: $0.27BaCl_2–0.73NaCl$ (1); $0.27BaCl_2–0.36NaCl–0.37KCl$ (2); $0.27BaCl_2–0.73KCl$ (3); and $0.27BaCl_2–0.36NaCl–0.37KCl$ [11] (4).

Table 1: Coefficients of (2) for molten $BaCl_2–MCl$ systems.

Solvent	Temperature interval (K)	$A \pm \Delta A$	$-(B \pm \Delta B) \cdot 10^{-3}$	$\Delta(\ln S)$	R^2	*S* at 973 K (m.f)
$0.27BaCl_2–0.73NaCl$	978–1083	2.35 ± 0.7	6.0 ± 0.7	0.07	0.98	0.021
$0.40BaCl_2–0.60NaCl$	910–1068	2.55 ± 0.2	5.20 ± 0.2	0.03	0.99	0.061
$0.27BaCl_2–0.36NaCl–0.37KCl$	799–1058	1.27 ± 0.1	4.38 ± 0.1	0.02	0.99	0.040
$0.27BaCl_2–0.73KCl$	963–1033	0.77 ± 0.7	3.86 ± 0.8	0.07	0.98	0.064

$$\Delta\bar{G}^{*}=\Delta\bar{H}^{*}-T\Delta\bar{S}^{*}=-RT\left(A+\frac{B}{T}\right) \qquad (4)$$

The conditional enthalpy ($\Delta H^{*}=-RB$) and entropy changes ($\Delta S^{*}=RA$) during the BaO dissolution are presented in Table 2.

One can see that substitution of sodium chloride on potassium chloride at the same $BaCl_2$ concentration reduces the endothermic effect of the BaO dissolution. For all solvents under study, the enthalpy changes during the BaO dissolution are smaller than the barium oxide melting enthalpy (58.47 kJ/mol [16]). This fact denotes the exothermal interaction between barium oxide and solvent particles at their mixing.

According to literature data [17], the solubility of such oxides as CaO and SrO in molten $MCl–CaCl_2$ and $MCl–SrCl_2$ increases with the reduction of the alkali metal cation radius (M^+). While the enthalpy of dissolution increases [17] indicating the same tendency as for barium containing molten systems (Tab. 2). In this connection, the decreasing of the lead oxide (II) solubility in molten $MCl–PbCl_2$ with substitution of cesium chloride on potassium chloride should be pointed out. As it was shown in [5], the solubility of lead oxide in molten $0.5KCl–0.5PbCl_2$ system at 806 K was about 8 mol.%, whereas in molten $0.713CsCl–0.287PbCl_2$ (with smaller content of lead chloride), 12 mol.% of oxide dissolved.

Probably the reduction of the radius of the alkali metal cation which located in the second coordinating area results in the decrease in the oxychloride ionic groupings stability.

For all the solvents under study, the XRD data of frozen fusion after the experiment show the presence of Ba_4OCl_6. For example, Figure 3 shows the XRD data for frozen [$NaCl–BaCl_2$ eutectic + BaO (8 mol.%)] melt. The composition of molten solvent should change during the Ba_4OCl_6 solid-phase formation according to (5):

$$[Ba_2OCl_6^{4-}+2BaCl_6^{4-}+12M^{+}](\text{solution})= Ba_4OCl_6(\text{solid})+[12Cl^{-}+12M^{+}](\text{solution}). \qquad (5)$$

To confirm flowing reactions (1) and (5), the presence of proper compounds and ionic groupings in the melt should be certificated by Raman spectroscopy.

Table 2: Thermodynamic characteristics of BaO solubility in molten chlorides.

Solvent	**ΔH^* (kJ/mol)**	**ΔS^* (J/(mol·K))**
$0.27BaCl_2–0.73NaCl$	49.9 ± 5.8	19.5 ± 5.8
$0.27BaCl_2–0.36NaCl–0.37KCl$	43.2 ± 0.8	21.2 ± 0.8
$0.27BaCl_2–0.73KCl$	36.3 ± 5.8	10.5 ± 6.6
$0.40BaCl_2–0.60NaCl$	32.0 ± 1.7	10.0 ± 1.7

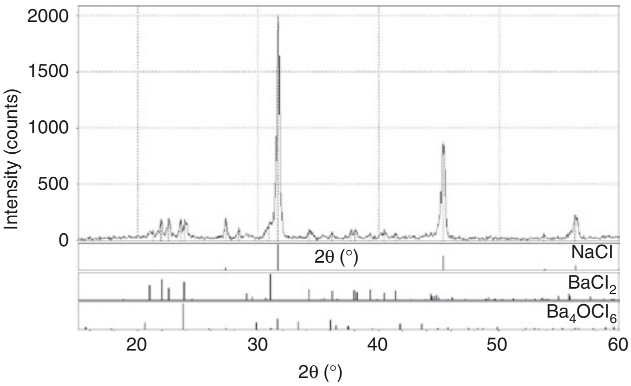

Figure 3: XRD data for frozen [$NaCl–BaCl_2$ eutectic + BaO (8 mol.%)] melt.

The Raman spectrum of $NaCl–BaCl_2$ eutectic melt is shows in Figure 4. In addition to the intense Rayleigh wing scattering, the band of small intensity in the area of 210 cm^{-1} is observed. This band we attributed to a symmetric valence vibration of the [$BaCl_6$] ionic groupings [12]. The location of the band in molten $NaCl–BaCl_2$ shifts toward larger frequencies as compared with that in molten $NaCl–KCl–BaCl_2$ [12]. It can be due to the strengthening of the force constant of Ba–Cl bond in [$BaCl_6$] ionic grouping when substituting of potassium cation on sodium cation. The small intensity of the vibration band may be the evidence of the mainly ionic type of interaction in this grouping.

Figure 5 demonstrates the Raman spectrum of $NaCl–BaCl_2$ eutectic melt after the considerable BaO addition exceeding its solubility at this temperature. The vibration band at 210 cm^{-1}, corresponding to the [$BaCl_6$] ionic grouping vibration is not observed but new vibration bands that can be attributed to [Ba_2OCl_6] grouping [12] appear at the 300 cm^{-1} area. The disappearance of the vibration band at 210 cm^{-1} as barium oxide is added can be connected with the [$BaCl_6$] chloride groupings destruction in the presence of O^{2-} anions with a greater ionic potential as compared to the Cl^- anions. The analysis of the obtained spectroscopy

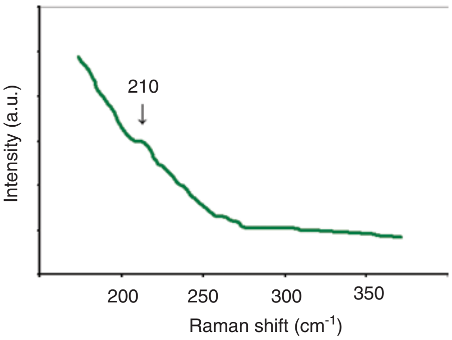

Figure 4: Raman spectra of molten $NaCl–BaCl_2$ eutectic, 943 K.

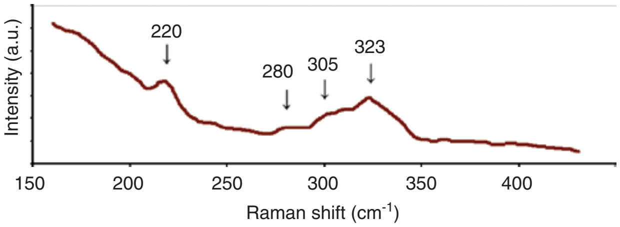

Figure 5: Raman spectra of molten NaCl–BaCl$_2$ eutectic with barium oxide addition (20 mol.%), 983 K.

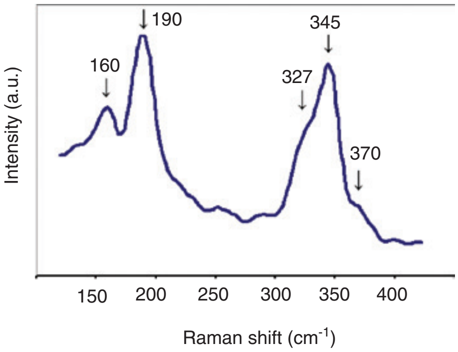

Figure 6: Raman spectra of solidified oxide-chloride mixture NaCl–BaCl$_2$–BaO after the high-temperature experiment.

results directly demonstrates the chemical mechanism of BaO dissolution in barium-containing chloride melts according to the (1). The vibration band at 220 cm^{-1} corresponds to the residue solid BaO [18] after interaction with the melt.

Figure 6 shows the Raman spectra of solidified oxide-chloride mixture NaCl–BaCl$_2$–BaO after the high-temperature experiment. The intensive vibration bands related to Ba$_4$OCl$_6$ [12] phase are observed. The disappearance of the BaCl$_2$ phase and the occurrence of the oxychloride Ba$_4$OCl$_6$ one confirm the chemical mechanism of oxide dissolution in molten NaCl–BaCl$_2$ eutectic.

4 Conclusion

The liquidus temperatures of (NaCl–BaCl$_2$)–BaO systems with different barium chloride concentration were determined by the thermal analysis methods. The barium oxide solubility in molten NaCl-BaCl$_2$ was determined as a function of temperature.

The same regularities of barium oxide dissolution in molten NaCl–BaCl$_2$, NaCl–KCl–BaCl$_2$, and KCl–BaCl$_2$ systems were revealed. The substitution of potassium chloride on sodium chloride was shown to result in slightly reduction of the barium oxide solubility in the melts with the same barium chloride content.

In situ Raman spectroscopic analysis provided direct evidence of chemical interaction between BaO and barium containing chloride melts.

Acknowledgments: The XRD-analysis was performed using the facilities of the Shared Access Centre “Composition of Compounds” (Institute of High Temperature Electrochemistry, Ural Branch of RAS).

References

[1] V. L. Cherginets, Oxoacidity: Reactions of Oxo-Compounds in Ionic Solvents, Elsevier Science, Amsterdam 2005.

[2] S.-L. Wang, W. Wang, S.-C. Li, and S.-H. Cao, Int. J. Miner. Metall. Mater. **17**, 791 (2010).

[3] P. S. Pershin, V. P. Batukhtin, N. I. Shurov, P. A. Arkhipov, and Y. P. Zaikov. J. Chem. Eng. Data **57**, 2811 (2012).

[4] Y. P. Zaykov, A. V. Isakov, I. D. Zakiryanova, O. G. Reznitskikh, O. V. Chemezov, et al. J. Phys. Chem. B **118**, 1584 (2014).

[5] P. A. Arkhipov, I. D. Zakiryanova, A. S. Kholkina, A. V. Bausheva, and A. O. Khudorozhkova, Z. Naturforsch. **70**, 851 (2015).

[6] A. V. Volkovich, Melts **4**, 280 (1991).

[7] E. V. Nikolaeva, A. L. Bovet, I. V. Korzun, and I. D. Zakiryanova, Rasplavy **1**, 78 (2014) [In Russian].

[8] N. M. Barbin, A. P. Pekar, V. N. Nekrasov, and L. Ye. Ivanovskii, Melts **2**, 87 (1992).

[9] B. Neumann, C. Kröger, and H. Jütter, Z. Elektrochem. Angew. Phys. Chem. **41**, 725 (1935).

[10] S. Boghosian, A. Godo, H. Mediaas, W. Ravlo, and T. Osvold, Acta Chem. Scand. **45**, 145 (1991).

[11] M. V. Solodkova, V. I. Zhuravlev, A. B. Volkovich, and D. S. Yermakov, Rasplavy **4**, 69 (2002) [In Russian].

[12] E. V. Nikolaeva, I. D. Zakiryanova, I. V. Korzun, A. L. Bovet, and B. D. Antonov, Z. Naturforsch. **70**, 325 (2015).

[13] A. Khokhryakov and A. M. Khokhlova, Melts **5**, 408 (1989).

[14] G. Brauer, Handbuch der Praparativen Anorganischen, Ferdinand Enke Verlag, Stuttgart 1975.

[15] E. Vortisch, Neues Jahrb. Mineral. Geol. Palaeontol. Beilageband **38**, 182 (1914).

[16] I. Barin, Thermochemical Data of Pure Substances, Part I; VCH Verlags Gesellschaft, Weinheim 1993.

[17] D. S. Yermakov, V. I. Zhuravlev, and A. B. Volkovich, Rasplavy **2**, 35 (2000) [In Russian].

[18] B. M. Weckhuysen, G. Mestl, M. P. Rosynek, T. R. Krawietz, J. F. Haw, et al. J. Phys. Chem. **102**, 3773 (1998).